

DYNAMIC ANALYSIS OF BEAM-SLAB HIGHWAY BRIDGES

W. S. Peterson and C. N. Kostem, Lehigh University

bb The findings of an analytical study on the determination of vehicle-induced dynamic response of highway bridge superstructures are presented. The investigation utilized the finite element displacement approach. In contrast to the traditional one-dimensional modeling, which assumes the superstructure to be a single beam, the superstructure is here assumed to be two-dimensional, a composition of discrete beam and slab elements. The reported investigation was carried out for a simply supported bridge superstructure with a $71\frac{1}{2}$ -ft span length and no skew. The system consists of six 24/45 prestressed concrete I-beams and a $7\frac{1}{2}$ -in. thick concrete deck. An AASHO HS20-44 design vehicle was simulated by using a constant force system in the dynamic analysis. Damping was neglected, and the bridge surface was assumed to be free of imperfections. Numerical studies were carried out for various lane loadings and various vehicular speeds. Deflection and bending moment time histories for beams and deflection contour graphs for the deck slab corresponding to the 50-mph vehicular speed are provided. Analytical results were compared with the data obtained from field tests performed on the actual bridge. A good correlation was observed. This paper does not include the experimental study, which is presented in another publication. Conclusions were drawn and reported based on this investigation. |AUTHOR|

•THE DYNAMIC RESPONSE of bridge superstructures to moving loads has been a problem of interest for many years and has been studied by many investigators. The induced dynamic behavior produces a response spectrum indicating stresses and deformations that may be greater or less than those of the static load case for a given configuration (5). Most early investigations were aimed at the definition of the resonance characteristics of the bridge superstructure. In these early studies the entire bridge superstructure, which is composed of several girders and a slab, was idealized as a single beam for the analytical determination of the dynamic response (2, 3). This simplified model will only predict the gross behavior of the overall bridge superstructure. To establish the dynamic interaction of the components of the superstructure requires that a more refined model be employed. For the reported investigation the finite element method is used in which the system is assumed to consist of beam and plate elements. Advantages of the finite element method over the single beam model are the following:

1. A more realistic model that treats the entire cross section as a plate with several stiffeners is obtained,
2. The dynamic behavior of the superstructure can be obtained in both longitudinal and lateral directions,
3. Individual beam behavior can be investigated,
4. The slab response is obtained,
5. Interaction between the various beams and the slab may be studied, and
6. Dynamic load distribution factors can be predicted.

BRIDGE IDEALIZATION

Numerical studies were performed using an existing bridge near Lehigh, Pennsylvania, as the test structure (4, 5). The superstructure has a 71½-ft simply supported span with no skew. A field test of this structure subjected to static and dynamic loadings has been reported (5). The bridge cross section is shown in Figure 1.

The bridge superstructure was discretized into 20 plate elements and 24 beam elements connected at the node points as shown in Figure 2 (1). A lumped mass model is used in which the contributions to each node point by the bridge slab, beams, parapet section, curb section, and truck are considered to be concentrated at the node points. Experiments carried out on prestressed concrete bridges indicated that damping is negligible for the short-term response spectrum (2, 3). Therefore, damping has been neglected in this study. In the analysis it was assumed that the bridge roadway was free of surface irregularities.

VEHICLE IDEALIZATION

In this investigation a constant force model is used. Consequently, each wheel group is idealized as a time-independent concentrated load that is linearly distributed to the nearest node points. The front, drive, and rear axle groups applied a total constant force of 10.2, 32.2, and 32.67 kip respectively. This model simulates the AASHTO HS20-44 design vehicle with spacing of 13.0 ft between front and drive axles and 20.4 ft between drive and rear axles.

ANALYTICAL RESULTS

Analytical studies were conducted for the following cases:

<u>Truck Position</u>	<u>Speed (mph)</u>
Lane 3	25
Lane 3	50
Lane 3	300
Lane 5	50

[The 300-mph speed was close to resonant speed of bridge superstructure (3).] For the sake of brevity, the discussions will be confined to the 50-mph lane 3 case. A non-dimensional distance ratio defined by the ratio of the (front-wheel distance)/(bridge length) is used to locate the truck position. Displacements in the upward direction and moments that produce tension on the bottom fibers are considered positive.

Displacement and bending moment time histories show the response of a particular node point or group of node points as the truck crosses the bridge. Figures 3 and 4 show the displacement and bending moment time histories of nodal points 22, 23, and 24 on beam B. The dynamic and static nodal point responses are plotted on these graphs so that comparisons can be made. The dynamic response appears as an almost symmetric oscillation about the smooth static response curve. In the 50-mph case, the vehicle traverses the span in approximately 1½ sec. At a distance ratio of 1.467, the rear axle of the vehicle leaves the span and the static response becomes zero. After a ratio of 1.467, the dynamic oscillations still persist and would theoretically continue indefinitely inasmuch as damping was not included in the analysis.

Figures 5 and 6 show the displacement and bending moment time histories of the midspan section (node points 3, 8, 13, 18, 23, and 28 located on beams F, E, D, C, B, and A respectively). Beams A, B, C, D, and E have maximum deflections in the downward direction and maximum moments that produce tension in the bottom fibers. Beam F deflects upward and is under a negative bending moment producing tension in the top fibers. This is caused primarily by the unsymmetrical lane 3 loading.

Figure 7 shows the midspan deflection diagrams for the 50-mph lane 3 loading. The diagrams are numbered in sequence and show the displaced shape of the cross section at midspan for distance ratio intervals of 0.1231 (0.12 sec). The cross section deflects

Figure 1. Cross section of test bridge.

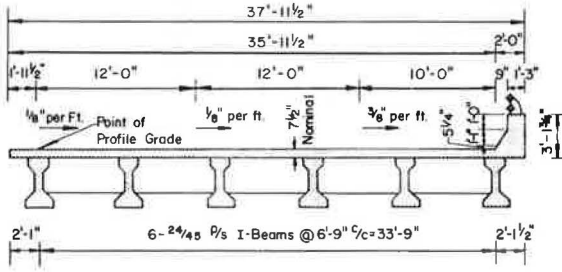


Figure 2. Finite element mesh.

30	25	20	15	10	5
29	24	19	14	9	4
28	23	18	13	8	3
27	22	17	12	7	2
26	21	16	11	6	1

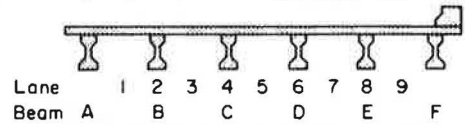


Figure 3. Displacement time history, 50-mph lane 3 case.

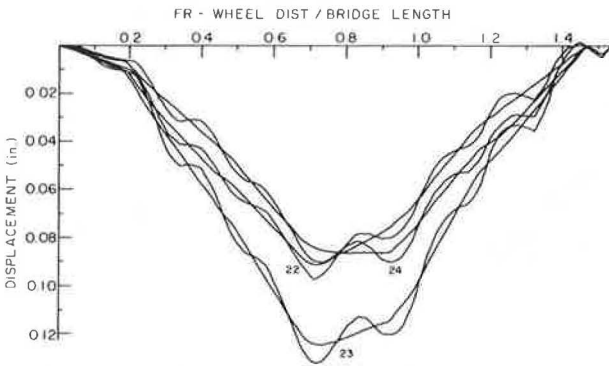


Figure 4. Bending moment time history, 50-mph lane 3 case.

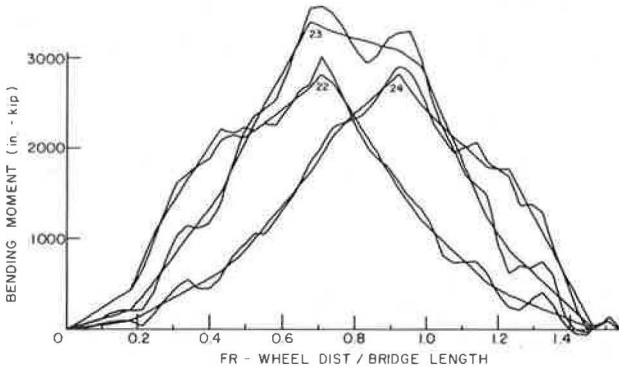


Figure 5. Displacement time history, 50-mph lane 3 case.

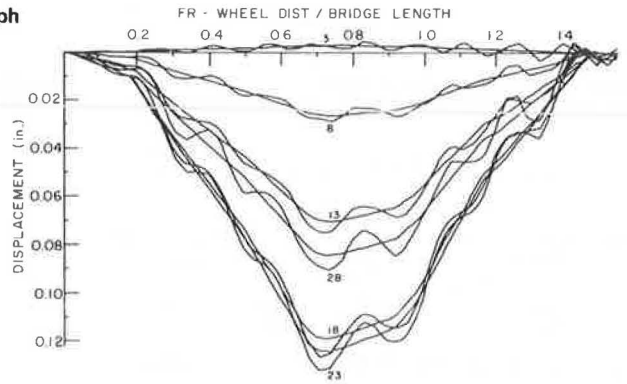


Figure 6. Bending moment time history, 50-mph lane 3 case.

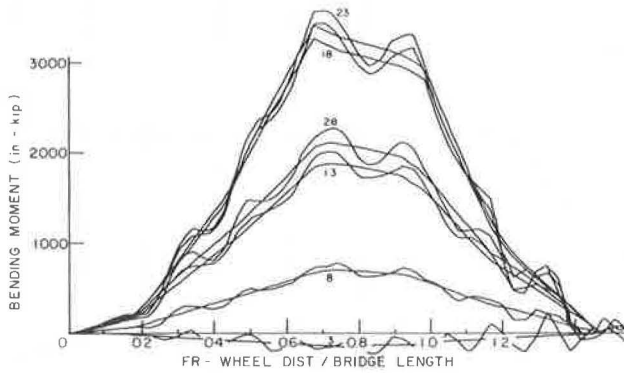


Figure 7. Displacement diagrams, 50-mph lane 3 case.

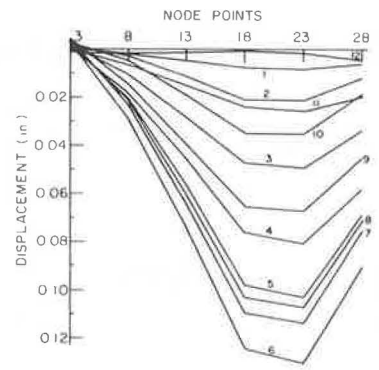


Figure 8. Displacement contours at distance ratio of 0.7076, 50-mph lane 3 case.

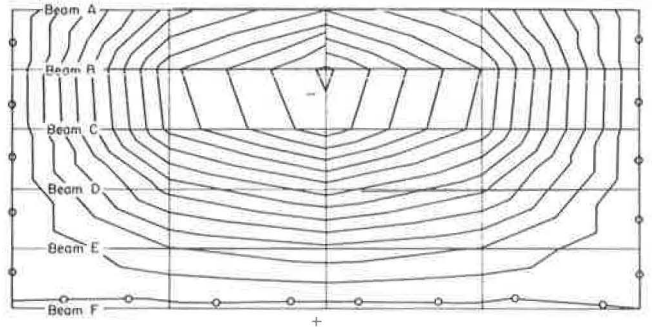


Figure 9. Displacement contours at distance ratio of 1.4153, 50-mph lane 3 case.

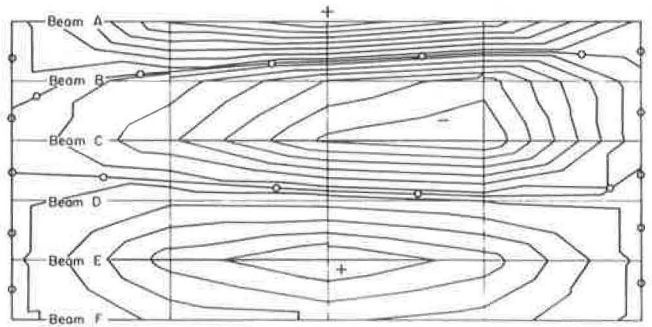


Figure 10. Displacement contours at distance ratio of 1.4462, 50-mph lane 3 case.

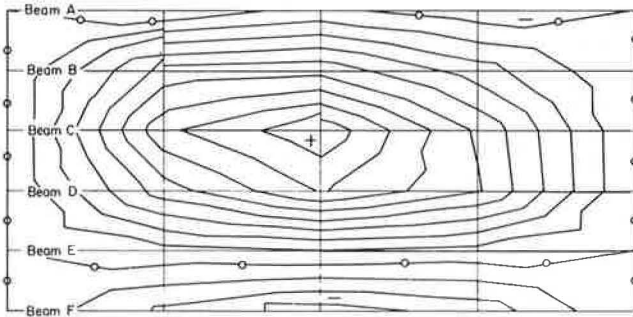


Table 1. Experimental and computed static midspan girder deflections and moments with corresponding ratios.

Beam	Node	Deflection (in.)			Moment (in.-kip)		
		Computed	Experimental	Computed/Experimental ^a	Computed	Experimental	Computed/Experimental ^b
A	28	-0.0842	-0.068	+1.24	+2,107	+1,905	+1.11
B	23	-0.1241	-0.090	+1.34	+3,350	+3,530	+0.95
C	18	-0.1188	-0.080	+1.48	+3,259	+3,168	+1.03
D	13	-0.0702	-0.052	+1.35	+1,879	+1,922	+0.98
E	8	-0.0260	-0.021	+1.24	+699	+772	+0.91
F	3	+0.0027	-0.004	-0.67	-150	+184	-0.82

^aAverage percentage of difference is 34.5.

^bAverage percentage of difference is 8.0.

Table 2. Computed midspan girder deflections and moments and corresponding computed and experimental dynamic load factors for the 50-mph lane 3 case.

Beam	Node	Deflections			Moments		
		Computed (in.)	Computed (DLF) _d	Experimental ^a (DLF) _d	Computed (in.-kip)	Computed (DLF) _e	Experimental ^b (DLF) _e
A	28	-0.0910	1.081	0.93	+2,282	1.083	1.06
B	23	-0.1321	1.064	1.02 ^c	+3,573	1.067	1.05
C	18	-0.1261	1.061	0.96	+3,431	1.053	1.03
D	13	-0.0749	1.067	0.97	+2,011	1.070	1.02
E	8	-0.0289	1.108	1.00	+773	1.106	1.21
F	3	+0.0046	1.704	1.33 ^c	-256	1.707	-2.24
			1.075	0.96		1.080	1.06

Note: DLF = dynamic load factor = $\frac{\text{maximum dynamic response}}{\text{maximum static response}}$; total (DLF)_d = $\frac{\sum \text{dynamic deflection}}{\sum \text{static deflection}}$ where $\Sigma^* = 0.86D_A +$

$D_B + D_C + D_D + D_E + 1.41 D_F$ (5); total (DLF)_m = $\frac{\sum \text{dynamic moment}}{\sum \text{static moment}}$.

^aFor 52.6 mph, lane 2.

^bFor 50.7 mph, lane 2.

^cValues were calculated by the authors and are different from those in an earlier report (5).

downward during the intervals 1 through 6 then upward as the truck leaves the bridge span during the intervals 6 through 12.

Displacement contours (i.e., lines connecting points of equal displacement) are shown in Figures 8, 9, and 10. A positive sign indicates a region of upward deflection, whereas a negative sign indicates a downward deflected region. The contours of zero displacement are marked with a 0. Figure 8 shows the displacement contours of the bridge superstructure at a distance ratio of 0.707 at which time the maximum displacement occurs at node 23. It can be noted that beam F is deflecting upward.

A contour displacement sequence (Figs. 9 and 10) is presented as the rear axle of the vehicle leaves the bridge. These figures illustrate the bridge vibration characteristics as the response of the superstructure approaches the state of free vibration. From the displacement contours it is apparent that the bridge deck vibrates in elliptical dish-shaped patterns with the major axis of the ellipse parallel to the longitudinal axis of the bridge. A line parallel to the major axis of the ellipse is seen to correspond to the first modal shape of a simply supported beam.

COMPARISON WITH EXPERIMENTAL RESULTS

The analytical results are compared to the Leighton Bridge field test results (4, 5). Experimental and analytical static deflection and moment values are given in Table 1. Theoretical results show beam F deflecting upward for a lane 3 loading, as in the case of an experimental lane 2 load, but opposite to an experimental lane 3 case. Beams A, B, C, D, and E exhibit deflection ratios greater than 1.0, indicating that the stiffness has been underestimated, whereas for beam F the stiffness has been overestimated. A deflection ratio is defined as the analytic result divided by the corresponding experimental result.

The computed dynamic midspan deflections and bending moments for the 50-mph lane 3 loading, along with the corresponding theoretical and experimental dynamic load factors, are given in Table 2. The total dynamic load factor, as defined in Table 2, provides a measure of the overall dynamic amplification of the static response. Beams not directly under the load (A, D, E, and F) tend to have higher amplification factors than those beams directly under the load (B and C). The maximum dynamic load factors exceed the AASHTO impact factor of 1.255 (6) and occur at beam F in both the experimental and analytical investigations. Experimental values obtained for the response of beam F may be in doubt due to the lack of sensitivity of the data logging equipment associated with measuring such small relative deflections. Also uncertainties may exist in the analytical model due to the difficulty in estimating the stiffness contribution made by the curb and parapet sections to beam F.

The average frequencies of vibration for the bridge superstructure are as follows:

1. Natural unloaded theoretical (single beam model) = 5.7 cps,
2. Loaded experimental (52.6 mph lane 2) = 5.5 cps, and
3. Loaded theoretical (finite element model, 50 mph lane 3) = 4.9 cps.

The loaded frequency is the frequency of vibration of the bridge superstructure when the mass of the loading vehicle is included in the system, whereas for the unloaded frequency the mass of the loading vehicle is not included in the system. The experimental and theoretical loaded frequencies were determined by finding the average loaded frequency of forced vibration for beam B. The natural unloaded frequency of free vibration was estimated by considering the entire superstructure cross section as a single beam (3). The single beam model gave the highest estimated frequency, whereas that from the finite element technique gave the lowest (1).

CONCLUSIONS

A two-dimensional finite element model rather than the one-dimensional single beam model was employed in the dynamic analysis of a beam-slab highway bridge superstructure. This two-dimensional model enabled the authors to obtain the static and dynamic response of the individual beams and slab sections. The analytical study including all the vehicle speeds shown previously and the available field test data has indicated the following:

1. The variation of the dynamic load factor is a nonlinear function of the vehicle speed.
2. The dynamic load factors for the exterior beams were consistently higher than those for the interior beams. Depending on the location of the vehicle, in some cases, they were also greater than the AASHO impact factor of $1 + \frac{50}{L + 125}$, which for the test bridge was 1.255.
3. Beams that are not directly under the load tend to have higher amplification of moment than those beams directly under the load. It should not be inferred from this that the maximum dynamic stresses necessarily occur in the beam with the maximum amplification factor. The maximum stress is, of course, a function of the maximum live load stress as well as the amplification factor.
4. The dynamic response of the beams tends to oscillate about the static response.

REFERENCES

1. Clough, R. W., and Felippa, C. A. A Refined Quadrilateral Element for Analysis of Plate Bending. Proc. Second Conf. on Matrix Methods in Structural Mechanics, Wright-Patterson AFB, Ohio, 1969, pp. 399-440.
2. Fenves, S. J., Veletsos, A. S., and Siess, C. P. Dynamic Studies on Bridges on the AASHO Road Test. HRB Spec. Rept. 71, 1962.
3. Linger, D. A., and Hulsbos, C. L. Dynamics of Highway Bridges. Iowa Eng. Exp. Station, Iowa State Univ., Proj. 370-S, Pt. I, July 1960.
4. Peterson, W. S., and Kostem, C. N. Dynamic Analysis of Highway Bridges Using the Finite Element Method. Fritz Eng. Laboratory, Lehigh Univ., Rept. 400.7, May 1972.
5. VanHorn, D. A., and Chen, C. H. Structural Behavior of a Prestressed Concrete I-Beam Bridge, Lehighon Bridge. Fritz Eng. Laboratory, Lehigh Univ., Rept. 349.4, Oct. 1971.
6. Standard Specifications for Highway Bridges. AASHO, 1969.